Results in Chemistry 4 (2022) 100503

Contents lists available at ScienceDirect

Results in Chemistry

journal homepage: www.sciencedirect.com/journal/results-in-chemistry

Facile synthesis, characterization, and catalytic activity of Cr(III) Schiff base complex immobilized on layered double hydroxide

Jagat Singh Kirar [a,*], Savita Khare [b]

[a] Department of Chemistry, Govt. P. G. College, In-Front of Sanjay Stadium, Guna, MP 473001, India
[b] School of Chemical Sciences, Devi Ahilya University, Takshashila Campus, Khandwa Road, Indore (M. P.) 452001, India

ARTICLE INFO

Keywords:
Layered double hydroxide (LDHs)
Heterogeneous catalyst
Schiff base complex
Toluene oxidation
Tert-butyl hydroperoxide

ABSTRACT

In the chemical industry, designing high-performance catalysts for the oxidation of aromatic hydrocarbon into value-added products such as benzaldehyde and benzoic acid is critical. In this study, the catalytic activity of chromium Schiff base complex supported on layered double hydroxide for the liquid phase oxidation of toluene was examined. The chromium Schiff base complex supported catalyst was synthesized by the intercalation method and abbreviated as LDH-[NAPABA-Cr(III)]. The obtained material was characterized by various physical techniques such as ICP-AES, XRD, FTIR, SEM, EDX, TEM, TGA, and EPR. The catalytic activity of the heterogenized Cr(III) Schiff base complex was tested for the oxidation of toluene using *tert*-butyl hydroperoxide as an oxygen source. Furthermore, the hot filtration experiment revealed that the LDH-[NAPABA-Cr(III)] was a heterogeneous catalyst that could be reused at least seven times without significant loss of catalytic activity.

1. Introduction

Selective oxidation of the C—H bond of toluene has drawn immense attention, because oxidation products benzaldehyde, benzoic acid, benzyl alcohol, and benzyl benzoate were useful in fine chemical industries, laboratories, pharmaceutical industries, and food industries [1]. Benzoic acid is commercially produced by partial oxidation of toluene with molecular oxygen (O_2) at 165 °C with acetic acid as solvent, in the presence of homogeneous cobalt and manganese naphthenates, but the conversion was only 15% [2,3]. This method suffers from its corrosive and environmentally unfriendly. Oxidation of toluene with molecular oxygen, hydrogen peroxide and *tert*-butyl hydroperoxide (*t*-BuOOH) is the preferred process for terminal oxidation [4,5]. Most of these catalysts are having certain drawbacks like difficulty in separation of catalyst at the end of reaction for reuse as well as decomposition during the catalytic reaction. Therefore, heterogenization of homogeneous metal complexes on insoluble support to develop new heterogeneous catalysts using various methods has attracted a lot of attention. Heterogeneous catalysts have a high surface area of the catalytically active sites to the reactants and have separation and recycling advantages compared to homogeneous catalysts. However, either leaching or low selectivity was the main problem regarding their applications as oxidation catalysts. Therefore, several researchers have worked extensively to design a suitable heterogeneous catalytic system for the oxidation of toluene [6–11].

Layered double hydroxides (LDHs) also known as hydrotalcite-like compounds, have the general formula $[M^{II}_{1-x}M^{III}_{x}(OH)_2]^{x+}.(A^{n-}_{x/n}).mH_2O$, where A^{n-} is the interlayer anion of charge n that leads to the electro-neutrality of LDH. The coefficient x is equal to the molar ratio $[M^{II}/(M^{II}+M^{III})]$, and m is the number of water molecules located in the interlayer region together with the anions [12]. Recently the LDHs have received intensive attention in intercalation chemistry [13], ion exchangers [14] and heterogeneous catalyst precursors [15–17]. LDH has also been studied extensively as strong support for the immobilization of a variety of transition metal complexes [18–21]. Recently, we have published Cu(II), Co(II), Mn(II) and Fe(III) Schiff base complexes immobilized on layered double hydroxide for the oxidation of toluene using TBHP as an oxidant [22,23].

The current research will concentrate on the solvent-free catalytic oxidation of toluene over LDH-supported heterogeneous catalysts, LDH-[NAPABA-Cr(III)], with *tert*-butyl hydroperoxide as an oxidant. To optimize the reaction conditions for maximum conversion and selectivity, we investigated the effects of various solvents, oxidants, the molar ratio of TBHP to toluene, the quantity of catalyst, and the effect of temperature. A hot filter experiment was also used to investigate metal leaching, as well as a plausible mechanism.

* Corresponding author.
E-mail address: j.skirar007@gmail.com (J. Singh Kirar).

https://doi.org/10.1016/j.rechem.2022.100503
Received 8 June 2022; Accepted 29 August 2022
Available online 6 September 2022

2. Experimental section

2.1. Chemical and physical characterization

Zinc nitrate hexahydrate ($Zn(NO_3)_3{\cdot}6H_2O$), aluminium nitrate nonahydrate ($Al(NO_3)_3{\cdot}9H_2O$, sodium hydroxide, 4-amino benzoic acid, 2-hydroxy-1-naphthaldehyde, toluene and 70% commercial aqueous solution of TBHP were of analytical grade E. Merck. Chromium chloride hexahydrate ($CrCl_3{\cdot}6H_2O$) is purchased from Central Drug House (CDH). Toluene E. Merck was checked by gas chromatography (G.C.) to ensure that no oxidation products were present in the substrate. E. Merck also supplied the 70% commercial aqueous solution of TBHP. A 74% TBHP in toluene stock solution was made by extracting 50 ml of commercial TBHP (70% in water) into 12 ml of toluene. The saturation of the aqueous layer with NaCl promotes phase separation. The organic layer is dried over $MgSO_4$, filtered, and kept at 5 °C. In this solution, the molar ratio of TBHP to toluene is 3 [24].

The Powder X-ray diffraction (XRD) patterns of the samples were recorded on a Rigaku diffractometer in the 2θ range of 3°–70° using CuKα radiation (λ = 1.5418 Å) at a scanning speed 2° per minute with step size 0.02°. Scanning electron microscopy (SEM) measurements were performed using a JEOL JSM 6100 electron microscope, operating at 20 kV. The Fourier transform infrared (FTIR) spectra were recorded on Perkin Elmer model 1750 in KBr. Transmission electron microscope (TEM) micrographs of the samples were recorded on a Tecnai G^2 20 microscope. The electron paramagnetic resonance (EPR) spectrum was recorded on a JES-FA200 ESR, X band spectrometer operated at a microwave frequency of 9.65 GHz at room temperature. The g value is reported relative to a 2, 2-diphenyl-1-picrylhydrazil (dpph) standard with g = 2.0036. Thermo-gravimetric analysis (TGA) was conducted on a Shimadzu TGA-50 system in the range 298–1023 K, at a heating rate of 10 °C min^{-1}. The data were analysed with the NORMOS-SITE program and the obtained parameters were fitted with respect to natural chromium. ThermoFischer Scientific, Flash smart V CHNS/O analyzer was used for the estimation percentage of C, H, N and O. Thermo Electron IRIS INTREPID II XSP DUO, inductively coupled plasma atomic emission spectroscopy (ICP-AES) was used for the estimation of chromium. The N_2 adsorption data, measured at 77 K by volumetric adsorption set-up (Micromeritics ASAP-2010, USA), were used to determine BET surface area. Analytical gas chromatography was carried out on a Shimadzu Gas Chromatograph GC-14B with dual flame ionization detector (FID) and attached Shimadzu printer having SE-30 ss column at 343 K. The products were identified by GC–MS (Perkin-Elmer Clasus 500 column; 30 mm × 60 mm).

2.2. Preparation of catalyst

2.2.1. Preparation of ligand {[NAPABA]}

The Schiff base ligand [NAPABA] was synthesized by dissolving 4-amino benzoic acid (10 mmol) into a 50 ml methanolic solution of NaOH (20 mmol) followed by the methanolic solution of 2-hydroxy-1-naphthaldehyde (10 mmol) in 1:1 M ratio, immediately the mixture became yellow due to imines formation. The resulting mixture was refluxed for 3 h with continuous stirring under a nitrogen atmosphere. The yellow product was filtered off, washed with methanol followed by acetonitrile and then dried at 333 K overnight. The obtained ligand was characterized by elemental analysis, CHNO and FTIR spectroscopy. The elemental percentage of CHNO for $C_{18}H_{12}NNaO_3$: Anal. found: C, 70.17%; H, 4.13%; N, 4.75%, O, 16.09%. Calc. found: C, 69.01%; H, 3.86%; N, 4.47%, O, 15.32% FTIR (KBr pellet: cm^{-1}): 3381 (br), 1721 (w), 1607 (m), 1547 (m), 1435 (w).

2.2.2. Preparation of neat Cr(III) Schiff base complex

The Cr(III) complex was synthesized by dissolving [NAPABA] ligand (10 mmol) into 100 ml of methanol and then immediately $CrCl_3{\cdot}6H_2O$ (5 mmol) was added and the mixture was kept under continuous stirring for 4 h at room temperature. After 4 h the greenish brown precipitate of NAPABA-Cr(III) complex was formed which was filtered, washed with petroleum ether and dried in air. The obtained complex was characterized by elemental analysis, CHNO and FTIR spectroscopy. The elemental percentage of CHNO for $C_{36}H_{26}CrN_2Na_2O_8$: Anal. Found: C, 62.46%; H, 3.31%; N, 4.13%, O, 18.07%. Calc. found: C, 60.68%; H, 3.68%; N, 3.93%, O, 17.93%. FTIR (KBr pellet: cm^{-1}): 3373(br), 1608 (m), 1581(m), 1476(w), 1409(m), 738(w), 553(w).

2.3. Preparation of heterogeneous catalyst

The heterogeneous catalyst was prepared in three steps. In the first step: 4-amino benzoic acid intercalated layered double hydroxide {LDH-[NH_2-C_6H_4COO]} was prepared by the co-precipitation method [24]. For synthesizing {LDH-[NH_2-C_6H_4COO]} a solution of zinc(II) nitrate hexahydrate (14.8 g) and aluminium(III) nitrate nonahydrate (6.25 g) in decarbonized water was prepared by taking Zn-Al molar ratio of 3 and then a solution of 4-amino benzoic acid (10.86 g) and NaOH (7.8 g) in decarbonized water was added to this solution with constant stirring. Immediately, a gel-like solution was formed, which was digested for 48 h at 348 K. After cooling, the off-white product was separated by filtering, washed with water, followed by methanol, and dried overnight at 333 K.

In the second step: ligand [LDH-NAPABA] was synthesized by the reaction of LDH-[NH_2-C_6H_4COO] with a methanolic solution of 2-hydroxy-1-naphthaldehyde (1:1 M ratio). The reaction mixture was refluxed for three hours under a nitrogen atmosphere. The yellow product was isolated by filtration and washed with methanol followed by acetone and acetonitrile, dried overnight at 333 K.

In the third step: The heterogeneous catalyst, LDH-[NAPABA-Cr(III)] was prepared by complexation of Cr(III)) with LDH-NAPABA ligand. Typically, the LDH-NAPABA ligand was suspended in 50 ml methanol and a solution of $CrCl_3{\cdot}6H_2O$ in 50 ml methanol was added to it with continuous stirring. The mixture was refluxed for 4 h under a nitrogen atmosphere. After cooling greenish brown solid was filtered and washed with methanol. The resulting solid was Soxhlet extracted using methanol followed by acetone, dichloromethane and acetonitrile to remove complex present on the surface of LDH and dried at 333 K.

Table.1
Chemical composition and physical data of various compounds.

Catalyst	Metal contents* (%)	Elemental composition (Wt %)#						BET surface area (m^2/g)	Pore volume (cm^3/g)	Pore size (Å)	d-spacing (Å)
		Zn	Al	C	O	N	Cr				
LDH-[NH_2-C_6H_4COO]	–	26.39	7.73	32.49	29.12	4.27	–	6.92	0.017	100.90	15.71
LDH-[NAPABA-Cr (III)]	4.43	16.41	6.24	45.05	23.17	3.67	5.46	29.93	0.121	46.51	22.21
LDH-[NAPABA-Cr (III)]a	4.39	16.30	6.12	44.95	23.14	4.05	5.38	27.81	0.097	39.97	22.21

*ICP-AES analysis; #EDX analysis; a: after catalytic reaction.

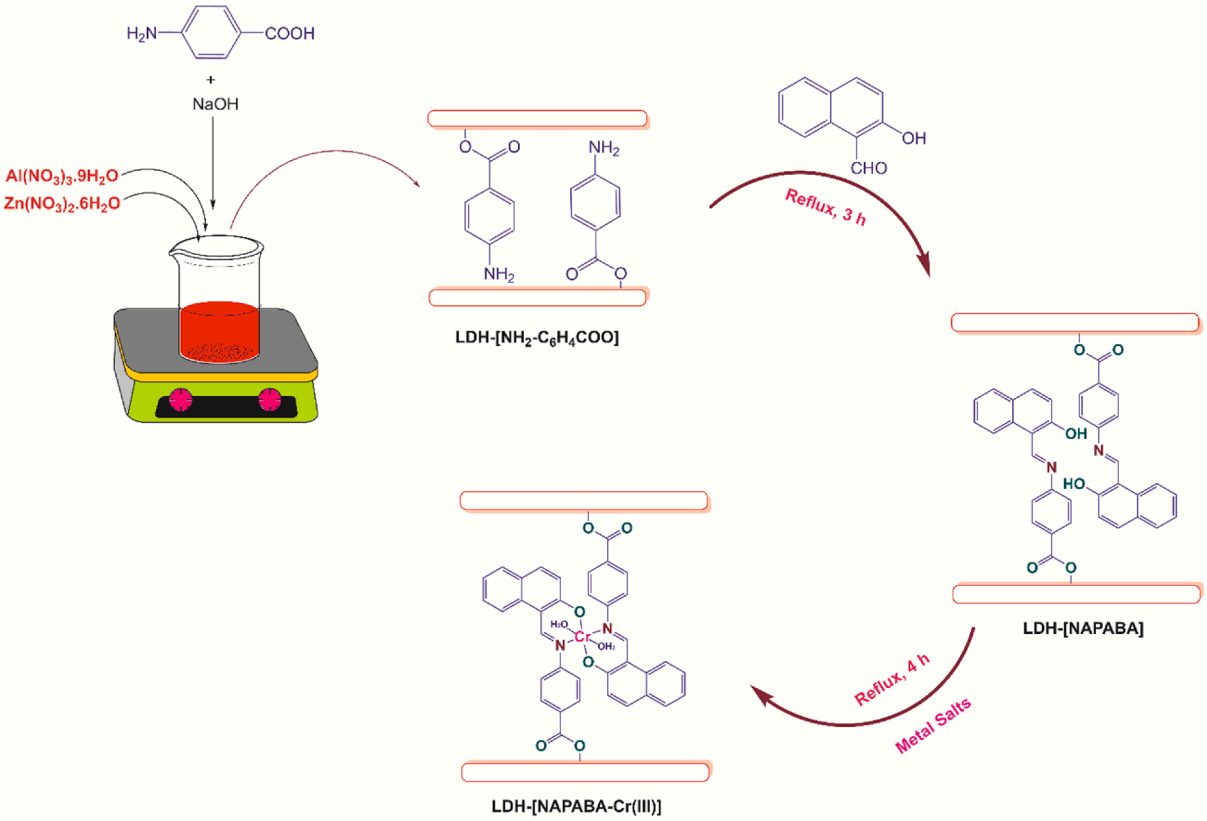

Scheme 1. Synthetic route of LDH-[NH_2-C_6H_4COO], LDH-[NAPABA] and LDH-[NAPABA-Cr(III)].

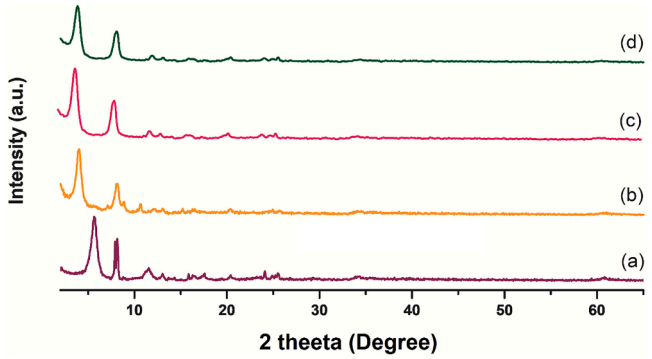

Fig. 1. XRD pattern of (a) LDH-[NH_2-C_6H_4COO], (b) LDH-[NAPABA], (c) LDH-[NAPABA-Cr(III)] and (d) reused LDH-[NAPABA-Cr(III)].

2.4. Catalytic oxidation of toluene

The oxidation reaction is carried out, in a two-neck round bottom flask fitted with a reflux condenser and mechanical stirrer. Flask is loaded with 14 mmol of toluene and 0.1 g of catalyst. The mixture was heated in an oil bath to 393 K before 42 mmol TBHP was added. For 5 h, the mixture was stirred at a constant temperature. The solid catalyst was separated from the reaction mixture at the end of the reaction. G. C. quantitatively examined the liquid layer using an SE-30 ss column at 343 K. The GC–MS was used to identify the products, which indicated that the primary compounds generated in the reaction were benzoic acid and benzaldehyde. The selectivity was determined in relation to the converted toluene.

3. Results and discussion

3.1. Characterization of catalysts

3.1.1. Estimation of metal contents

ICP-AES was used to determine the metal contents of a heterogeneous catalyst, LDH-[NAPABA-Cr(III)], and the findings show that the catalyst contains 4.43% chromium. The elemental composition of LDH-[NH_2-C_6H_4COO] and LDH-[NAPABA-Cr(III)] was determined using EDX analysis. The EDX analysis reveals the presence of carbon, oxygen, nitrogen, aluminium, and zinc in LDH-[NH_2-C_6H_4COO]. The catalyst LDH-[NAPABA-Cr(III)] comprises carbon, oxygen, nitrogen, as well as aluminium, zinc, and chromium. The results are listed in Table 1. The existence of these components in LDH-[NAPABA-Cr(III)] verifies the formation of the catalyst. The EDX analysis is depicted in Fig. S1 in Supplementary materials. The synthetic route of LDH-[NH_2-C_6H_4COO], LDH-NAPABA ligand, and LDH-[NAPABA-Cr(III)] catalysts is shown in Scheme 1.

Fig. 1 shows the XRD patterns of LDH-[NH_2-C_6H_4COO], LDH-[NAPABA], LDH-[NAPABA-Cr(III)], and reused LDH-[NAPABA-Cr(III)], which reveal the existence of two strong and narrow diffraction lines corresponding to (0 0 3) and (0 0 6) reflections of a crystalline ZnAl-LDH phase [25–27]. LDH-[NH_2-C_6H_4COO] exhibits the most intense basal reflection at (0 0 3) plane with a d-spacing of 15.71 (Table 1). In LDH-[NAPABA-Cr(III)] the basal spacing of the (0 0 3) plane rises from 15.71 to 22.21. The metal Schiff base complex had no effect on the LDH structure during intercalation [28]. The appearance of (0 0 3) and (0 0 6) reflections confirm the ZnAl-LDH material's layered structure [29]. The absence of any additional peak owing to other phases or impurities indicates that the phase is pure ZnAl-LDH. Additionally, no change in the typical reflections corresponding to the (1 1 0) plane, which is associated with the atomic distribution density and depends on the Zn/Al molar ratio, is verified. The increase in gallery height indicates a good

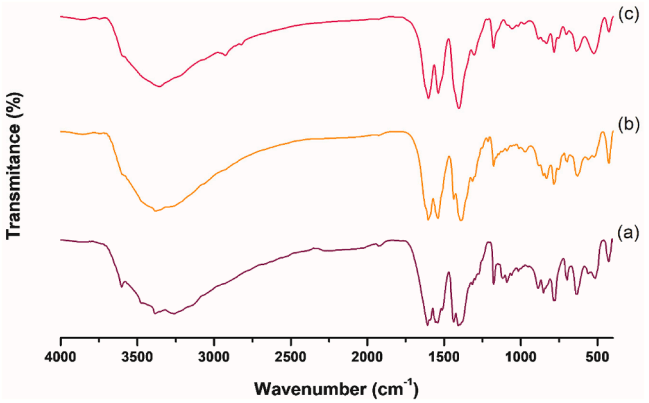

Fig. 2. FTIR spectra of (a) LDH-[NH_2-C_6H_4COO], (b) LDH-[NAPABA] and (c) LDH-[NAPABA-Cr(III)].

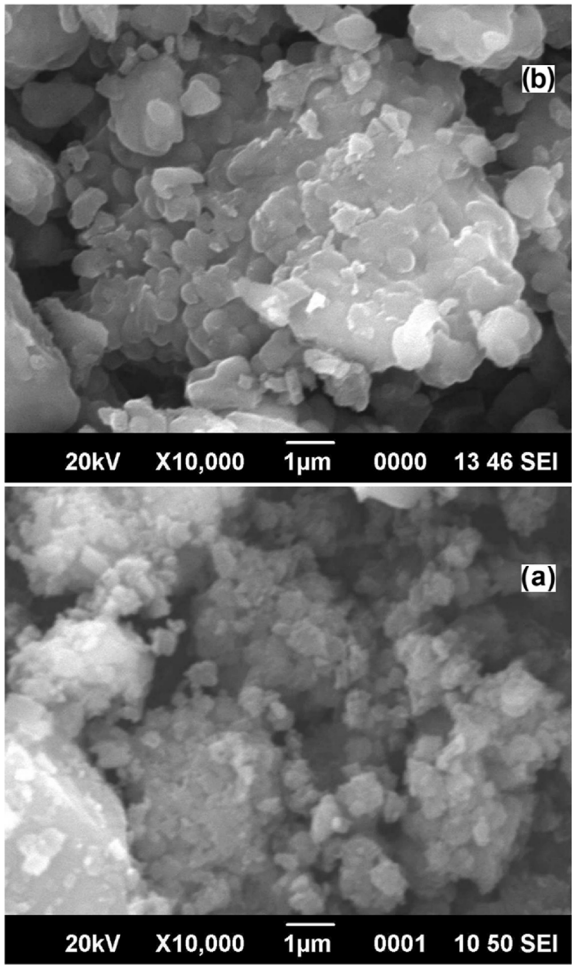

Fig. 3. SEM images of (a) LDH-[NH_2-C_6H_4COO], and (b) LDH-[NAPABA-Cr(III)].

agreement with the effective chromium Schiff base complex intercalated in the LDH host layers. After seven cycles, the d-spacing of the reused LDH-[NAPABA-Cr(III)] catalyst, did not alter considerably (Table 1 and Fig. 1(c).

3.1.3. FT-IR analysis

The FTIR spectrum of LDH-[NH_2-C_6H_4COO], LDH-[NAPABA] and LDH-[NAPABA-Cr(III)] were recorded in the range 4000 to 400 cm^{-1}

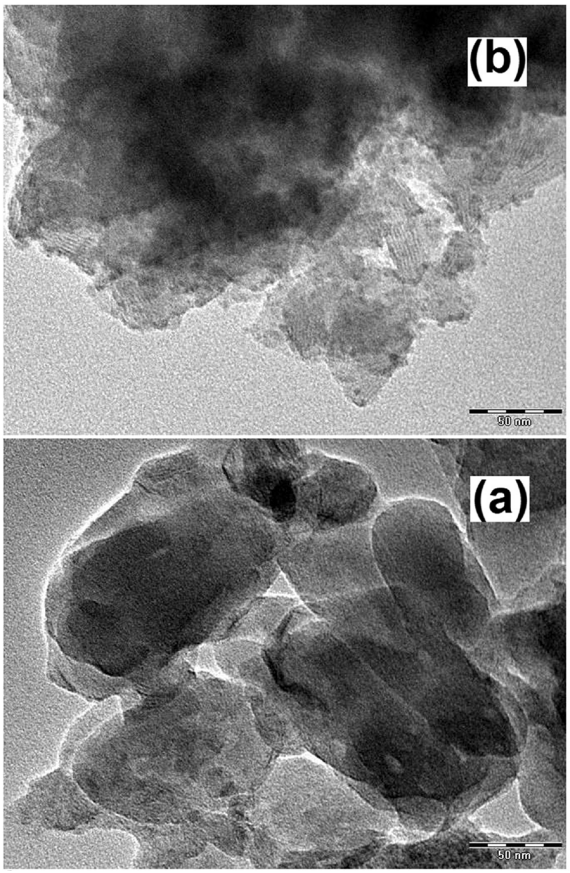

Fig. 4. TEM images of (a) LDH-[NH_2-C_6H_4COO], and (b) LDH-[NAPABA-Cr(III)].

shown in Fig. 2. The stretching mode of OH groups is responsible for the broad absorption bands at 3280–3400 cm^{-1} in the spectra of LDH-[NH_2-C_6H_4COO]. The bands at 1608 and 1298–1315 cm^{-1} were assigned owing to bending and stretching vibrations of H—O—H and NO_3^-, which were found in the interlayers of LDH, respectively [30]. The absorption bands below 1016 and 425–553 cm^1 are caused by LDH's M–O and O–M–O vibration modes [31] In the spectra of LDH-[NAPABA-Cr(III), an extra band at 1610 cm^{-1} is due to imine C═N stretching, while bands at 755 and 561 cm^{-1} are due to Cr-N and Cr-O stretching frequencies, respectively.

3.1.4. SEM analysis

The morphology of LDH-[NH_2-C_6H_4COO] and LDH-[NAPABA-Cr (III)] was studied by scanning electron microscopy shown in Fig. 3. In SEM images, the presence of flake-like aggregates on both the substrate and the catalysts demonstrated that the particles of LDH-[NH_2-C_6H_4COO] were not destroyed during the intercalation of the metal Schiff base complex.

3.1.5. BET surface area analysis

The surface area of heterogeneous catalysts is an essential parameter in catalysis. As a consequence, the surface area of the LDH-[NH_2-C_6H_4COO] and LDH-[NAPABA-Cr(III)] was measured using BET surface area analysis. Table 1 summarises the findings. The surface areas of LDH-[NH_2-C_6H_4COO] and LDH-[NAPABA-Cr(III)] are 6.92 [32] and 29.93 m^2g^{-1}, respectively. The pore volume and pore size of support are 0.017 (cm^3/g) and 100.90 (Å) respectively. Following the intercalation of the chromium Schiff base complex into the LDH host layer, the pore volume increases to 0.121 (cm^3/g) while the pore size decreases to 46.51 (Å). The reason for the increase in surface area of catalysts in

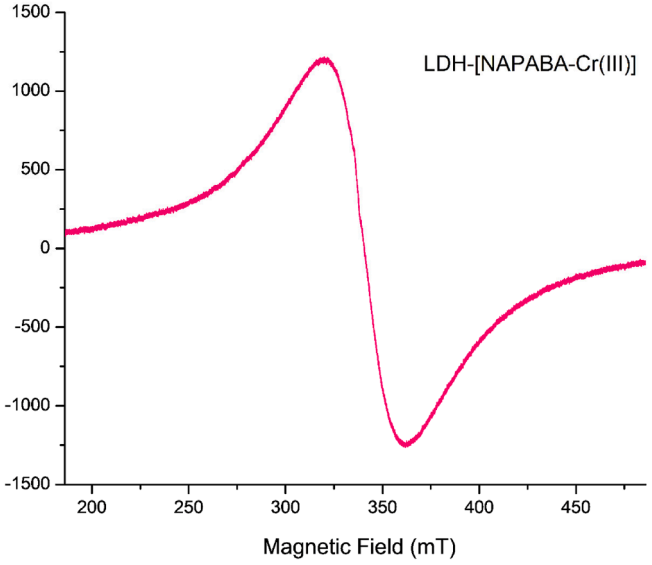

Fig. 5. EPR spectrum of LDH-[NAPABA-Cr(III)] catalyst.

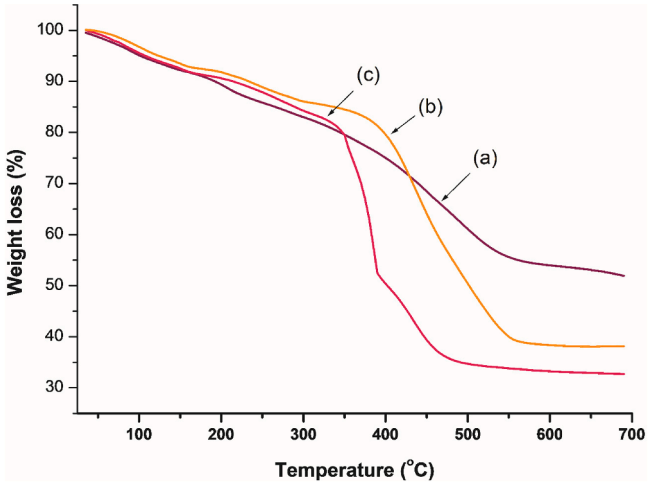

Fig. 6. TGA curves of (a) LDH-[NH_2-C_6H_4COO], (b) LDH-[NAPABA] and (c) LDH-[NAPABA-Cr(III)].

contrast to LDH-[NH_2-C_6H_4COO] was the intercalation of bigger complex molecules into the LDH layers, which resulted in layer expansion.

3.1.6. TEM analysis

TEM examination was used to examine the microstructure of LDH-[NH_2-C_6H_4COO], LDH-[NAPABA-Cr(III)] shown in Fig. 4. It was found that materials contain aggregates with a flake-like structure. TEM analysis was used to calculate the particle size of support and heterogeneous catalysts, which ranged from 5 to 20 nm and agreed well with the results of the XRD examination.

3.1.7. EPR analysis

The geometry and oxidation state of the chromium Schiff base complex was determined by EPR analysis. The X band EPR spectrum of LDH-[NAPABA-Cr(III)] catalyst was obtained at room temperature. A single peak at 320 mT can be seen in the EPR spectrum of the chromium Schiff base complex depicted in Fig. 5. Furthermore, the spectrum shows a g value of 1.947 with a g_{iso} of 2.07, indicating the existence of chromium metal ions in the +3 oxidation state with three unpaired d-orbitals. The EPR parameters for the Cr(III) complex are suggested in octahedral geometry [33].

Table 2
Catalytic activity support, homogeneous and heterogeneous catalysts in the oxidation of toluene.

Compounds	Oxidant/ Solvent	Toluene conversion (%)	Selectivity (%)		TON
			BA	BZ	
No Catalyst	TBHP /Solvent-free	–	–	–	–
LDH-[NH_2-C_6H_4COO]	TBHP /Solvent-free	–	–	–	-
NAPABA-Cr(III)	TBHP /Solvent-free	63.8	81.7	18.3	580
LDH-[NAPABA-Cr(III)]	TBHP/ Solvent-free	81.2	86.4	13.6	738

BZ: benzaldehyde, BA: benzoic acid; TBHP: 74% TBHP in toluene; Reaction conditions: toluene (14 mmol); TBHP (42 mmol), catalyst (100 mg), temperature (393 K), time 5 h. TON: turnover number.

3.1.8. TGA analysis

TGA is used to assess the thermal stability of LDH-[NH_2-C_6H_4COO], LDH-[NAPABA] and LDH-[NAPABA-Cr(III)] shown in Fig. 6 and Table S1. The TGA curves of LDH-[NH_2-C_6H_4COO] indicate the elimination of adsorbed water as the initial weight loss at temperatures ranging from 25 to 150 °C. The second weight loss occurs between 200 and 500 °C due to the breakdown of the brucite-like layer and the elimination of interlayer benzoate anions. Whereas the LDH-[NAPABA-Cr(III)] TGA curve indicates the initial weight loss at temperatures ranging from 25 to 175 °C, which is related to the elimination of adsorbed water. The partial dihydroxylation of the double hydroxide layers is responsible for the second weight loss seen between 213 and 330 °C. The complete degradation of the metal complex caused the third weight loss in the temperature range 325–530 °C. The TGA curves show that the catalysts are stable up to 500 °C.

3.2. Catalytic properties of LDH-[NAPABA-Cr(III)] catalyst

The oxidation of toluene using *tert*-butyl hydroperoxide as an oxidant is examined to study the catalytic activity of the LDH-[NAPABA-Cr(III)] catalyst. We have also examined the support, LDH-[NH_2-C_6H_4COO], homogeneous catalysts, NAPABA-Cr(III), and heterogeneous catalyst LDH-[NAPABA-Cr(III)] under identical experimental conditions. Table 2 summarises the findings. It is observed that, in the absence of the catalyst, no oxidation products are produced, showing that auto-oxidation does not occur. In the case of support also, no oxidation products are formed. It is clear that the support is catalytically inactive. The homogeneous catalyst, NAPABA-Cr(III) and heterogeneous catalyst LDH-[NAPABA-Cr(III)] has successfully oxidized toluene to, benzoic acid, and benzaldehyde with no oxidation products seen from the aromatic ring of the toluene. The results indicate that heterogeneous catalyst, LDH-[NAPABA-Cr(III)] gave excellent catalytic activity in comparison to homogeneous catalysts, NAPABA-Cr(III)because homogeneous catalysts are partially soluble in the reaction mixture. Therefore, less amount of catalyst is available for the oxidation reaction. Scheme 2 depicts the toluene oxidation catalyzed by the LDH-[NAPABA-Cr(III)]/TBHP system. The substrate conversion and selectivity were calculated from the given equations [34,35].

$$\text{Substrate conversion } (\%) = \text{Substrate converted (mmol)}/\text{Substrate used (mmol)} \times 100.$$

$$\text{Product selectivity } (\%) = \text{Product formed (mmol)}/\text{Substrate used (mmol)} \times 100.$$

$$\text{Turn over number} = \text{mmol of products}/\text{mmol of catalyst.}$$

Various parameters such as the effect of oxidants, effect of TBHP,

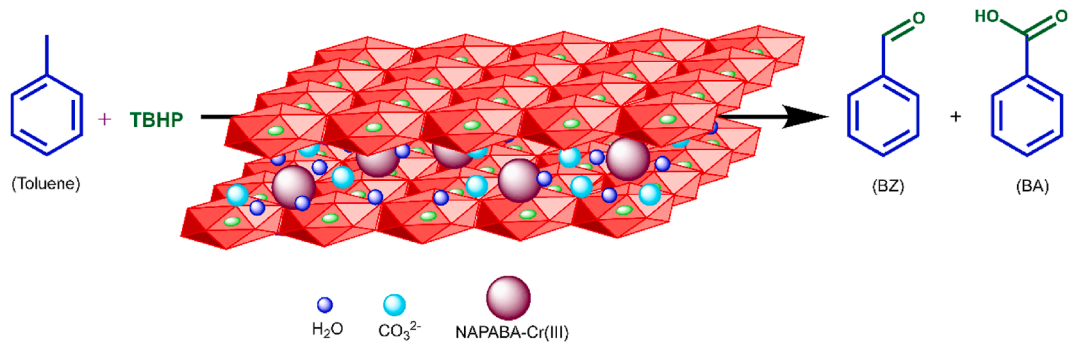

Scheme 2. Oxidation of toluene over LDH-[NAPABA-Cr(III)].

Table 3
Effect of oxidants and solvents for the oxidation of toluene over LDH-[NAPABA-Cr(III)] heterogeneous catalyst.

Entry	Oxidants	Solvents	Toluene Conversion (%)	Selectivity (%)		TON
				BA	BZ	
1	H_2O_2	Solvent-free	–	–	–	–
2	O_2	Solvent-free	37.3	77.9	22.1	339
3	70% TBHP	Solvent-free	48.5	72.8	27.2	441
4	TBHP	Solvent-free	81.2	86.4	13.6	738
5	TBHP	Acetonitrile	49.3	79.5	20.5	448
6	TBHP	Acetone	10.7	78.2	21.8	97
7	TBHP	Benzene	31.4	72.8	27.2	286
8	TBHP	Methanol	15.3	54.8	45.2	139

BZ: benzaldehyde, BA: benzoic acid; TBHP: 74% TBHP in toluene; Reaction conditions: toluene (14 mmol); TBHP (42 mmol), catalyst (100 mg), temperature (393 K), time 5 h.

effect of the amount of catalyst as well as reaction temperature have been studied for obtaining the maximum conversion of toluene.

The effects of various solvents, such as polar protic, polar aprotic, and non-polar, have been investigated in order to maximize toluene conversion shown in Fig. S2. The reactions were carried out using 100 mg LDH-[NAPABA-Cr(III)], 393 K, and TBHP to toluene molar ratio 3 for 5 h utilizing different solvents such as acetonitrile, acetone, benzene, and methanol. The results clearly show that polar protic solvents improved benzaldehyde selectivity whereas polar aprotic and non-polar solvents improved benzoic acid selectivity. The conversion of toluene was also shown to be reduced in the presence of polar protic, polar aprotic and non-polar solvents. It's because of the competition for active sites between solvent and substrate molecules, as well as the blockage of active sites by solvent molecules [24]. However, in the absence of any solvent, better selectivity and catalytic activity were detected than in the presence of any solvent.

The effects of several oxidants such as H_2O_2, O_2, 70% TBHP, and 74% TBHP in toluene were examined. The results are listed in Table 3. The conversion of toluene was lower 37.3% when molecular oxygen (O_2) was utilized as the oxidant because O_2 was easily expelled from the reaction mixture. When H_2O_2 was utilized as the oxidant, no conversion was detected because of its strong exothermic nature, which allowed it to disintegrate quickly and emit oxygen. Because of the interference of water in the reaction, the conversion of toluene was lower 48.5% with 70% TBHP, whereas 74% TBHP in toluene provided the highest conversion of toluene 81.2%. As a result, it was determined to be the optimal oxidant for our catalytic system.

Three different molar ratios of TBHP to toluene were used to examine the effect of TBHP concentration on toluene oxidation (1, 2, and 3) shown in Fig. S3. The results are summarised in Table 4. Initially, with TBHP to toluene molar ratio of 1, toluene conversion was found to be 22.8% at 353 K and 50 mg of catalyst. The conversion of toluene steadily increases to 36.5% when the TBHP to toluene molar ratio is increased from 1 to 3 at 353 K temperature and 50 mg catalyst amount. It is observed that the conversion of toluene increases with increasing TBHP to toluene molar ratio. Therefore, we performed the optimization at a TBHP to toluene molar ratio of 3. With increasing molar ratio of TBHP to toluene from 1 to 3, a toluene conversion of 39.7 to 81.2% was found at 393 K and 100 mg catalyst amount. Fig. S4 shows that if we increase the catalyst loading from 50 to 100 mg, the conversion of toluene increases

Table 4
Oxidation of toluene over LDH-[NAPABA-Cr(III)] at various conditions.

TBHP: toluene molar ratio	Catalyst Amount (mg)	Temperature (K)	Toluene conversion (%)	Selectivity (%)		TON
				BA	BZ	
1	50	353	22.8	45.8	54.2	414
2	50	353	31.4	56.4	43.6	571
3	50	353	36.5	68.9	31.1	664
3	100	353	49.5	74.3	25.7	450
3	100	373	67.1	85.9	14.1	610
3	100	393	81.2	86.4	13.6	738
1	100	393	39.7	77.1	22.9	361
2	100	393	62.9	82.5	17.5	572
3	50	393	35.2	76.2	23.8	640
3	75	393	47.6	71.5	28.5	573

BZ: benzaldehyde, BA: benzoic acid; TON: turnover number; time: 5 h.

Table 5
Comparison of toluene oxidation catalysts from the literature and our catalyst system.

Catalyst	Oxidant	Time (h)	Toluene conversion (%)	Selectivity of BA (%)	Ref.
Co-MOF-74@Mn-MOF-74-4	TBHP	6	22.4	0.9	[36]
Cu/Co-ZNC	TBHP	12	56.4	98.5	[6]
Cu/grapheme	H_2O_2	8	11.5	66.5	[7]
MnOx/SBA-15	TBHP	1	24.7	8.3	[37]
MnCo-MOF-74	TBHP	6	17.6	–	[38]
NDHPI-epoxy/Co-SBA-15	TBHP	7	29.9	89.3	[39]
Co-MC	TBHP	6	9.0	92.4	[40]
LDH-[NAPABA-Cr(III)	TBHP	7	81.2	86.4	Present work

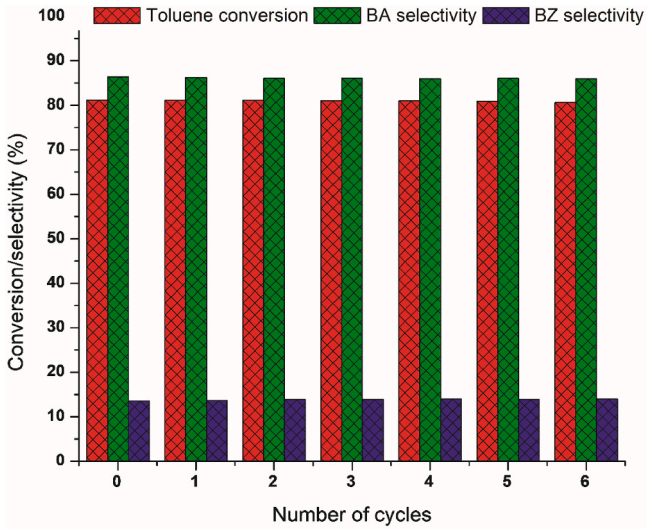

Fig. 7. Effect of recycling of LDH-[NAPABA-Cr(III)] catalyst on oxidation of toluene.

gradually from 35.2 to 81.2% with 76.2 to 86.2% selectivity to benzoic acid at 393 K after 5 h due to the high catalyst loading that provides a higher active center where the reaction occurs. This indicates that the larger the active site of the catalyst, the higher the catalytic activity. Table 5 compares our catalyst to previously reported catalysts. [36–40].

Similarly, it is observed that as the temperature increases from 353 to 373 K, the conversion of toluene increases from 49.5 to 81.2% shown in Fig. S5. With a further increase in temperature to 393 K, the conversion also increases to 81.2%. This may be due to the increase in the effective collision of the substrate at the higher temperature. Therefore, 393 K is considered the best reaction temperature. At all reaction temperatures, benzoic acid was the major product. Thus, overall optimal conditions for obtaining the maximum conversion of toluene are a TBHP to toluene molar ratio of 3, 100 mg catalyst, and a temperature of 393 K.

3.3. Recycling of the catalyst

The recycling experiment was carried out to investigate the stability and reusability of LDH-[NAPABA-Cr(III)] in toluene oxidation under optimized conditions. The catalyst was removed from the reaction mixture by filtering, washed multiple times with various solvents (methanol, acetone, and acetonitrile), and then dried at 333 K overnight to remove the adsorbed solvent molecules from the catalyst surface. The washed catalyst was then put through a series of catalytic runs. Within seven repeated cycles with the catalyst regeneration, the conversion of toluene steadily dropped from 81.2 to 80.6% as shown in Fig. 7. The loss of catalyst during washing after each cycle might be causing the reduction in toluene conversion. This indicates that the catalyst was stable during the catalytic process and may be recycled. XRD, BET surface area, and ICP-AES were used to further analyze the recovered catalyst (Table 1). The results reveal that there were no significant alterations after recycling. This suggests that the recovered catalyst was stable and reusable.

3.4. Hot filter experiment

A hot filter experiment was carried out under optimum reaction conditions to test the heterogeneity of the LDH-[NAPABA-Cr(III)] catalyst for the oxidation of toluene. To minimize re-adsorption of leached chromium onto the catalyst surface, the catalyst was filtered away after 1 h of reaction time in the first cycle at 393 K. After 1 h of the first cycle, the filtrate was poured back into the reaction flask, and the reaction was continued for the following 5 h. The gas chromatographic examination revealed that the conversion of toluene does not increase further; also, the reaction mixture did not exhibit any colour, indicating the lack of chromium, as determined by atomic absorption spectroscopy. The hot filter experiment results show that there was no metal leaching occurred during the catalytic process. This finding suggests that the catalyst was heterogeneous in nature.

3.5. Plausible mechanism for the toluene oxidation

The radical scavenger 2,6-di-*tert*-butyl-4-methylphenol (BHT) was employed as a quenching reagent in the quenching experiment to determine the mechanism of toluene oxidation. We did two sets of reactions at the same time. The first set of reactions was carried out without BHT, with toluene conversion increasing steadily for up to 5 h at 393 K. The second set of the reaction was conducted in the presence of BHT, with BHT being introduced after 2 h of reaction and the reaction continuing for another 5 h. The conversion of toluene did not increase with the addition of BHT, according to gas chromatographic analyses. The radical scavenger captures the free radical generated during the oxidation reaction, causing the reaction to cease. The quenching experiment shows that the oxidation reaction takes place through a free-radical pathway.

The aforementioned experiment and published literature were used to develop a plausible mechanism [41]. A plausible mechanism for the oxidation of toluene over the LDH-[NAPABA-Cr(III)] catalyst has been suggested in Scheme 3. Firstly, when *t*-BuOOH coordinates to the Cr(III) metal center give rise to chromium hydroperoxide species, which on decomposition leads to the formation of *tert*-butoxy radical (*t*-BuO•) and chromium hydroxide species. Then chromium hydroxide species again interact with another oxidant molecule (*t*-BuOOH) and generate chromium hydroperoxide species and water molecule. Then, the Cr-O bond of chromium hydroperoxide species is broken, resulting in the regeneration of the catalyst and the produces *tert*-butylperoxy radicals (*t*-BuOO•). This *tert*-butylperoxy radicals react with toluene in the second stage to generate *tert*-butylperoxytoluene. The *tert*-butylhydroxytoluene is highly unstable, hence decomposed to benzaldehyde by the elimination of *tert*-butanol. Benzaldehyde on further oxidation converted to benzoic acid.

4. Conclusions

In this study, we explored the synthesis, characterization, and catalytic activity of LDH-[NAPABA-Cr(III)] for the solvent-free oxidation of toluene with *tert*-butyl hydroperoxide as an oxidant. The heterogeneous catalyst shows a maximum 81.2% conversion of toluene with 86.4% benzaldehyde selectivity under optimized reaction conditions. The hot filter experiment suggested that the catalyst is stable and recyclable up to seven times without any significant loss of catalytic activity. Furthermore, a free-radical reaction preceded the oxidation of toluene. The octahedral geometry of the Cr(III) Schiff base complex was elucidated by the EPR parameters.

CRediT authorship contribution statement

Jagat Singh Kirar: Conceptualization, Data curation, Formal analysis, Investigation, Methodology, Software, Writing - original draft, Writing - review & editing. **Savita Khare:** Conceptualization, Supervision, Writing - review & editing.

Declaration of Competing Interest

The authors declare that they have no known competing financial interests or personal relationships that could have appeared to influence the work reported in this paper.

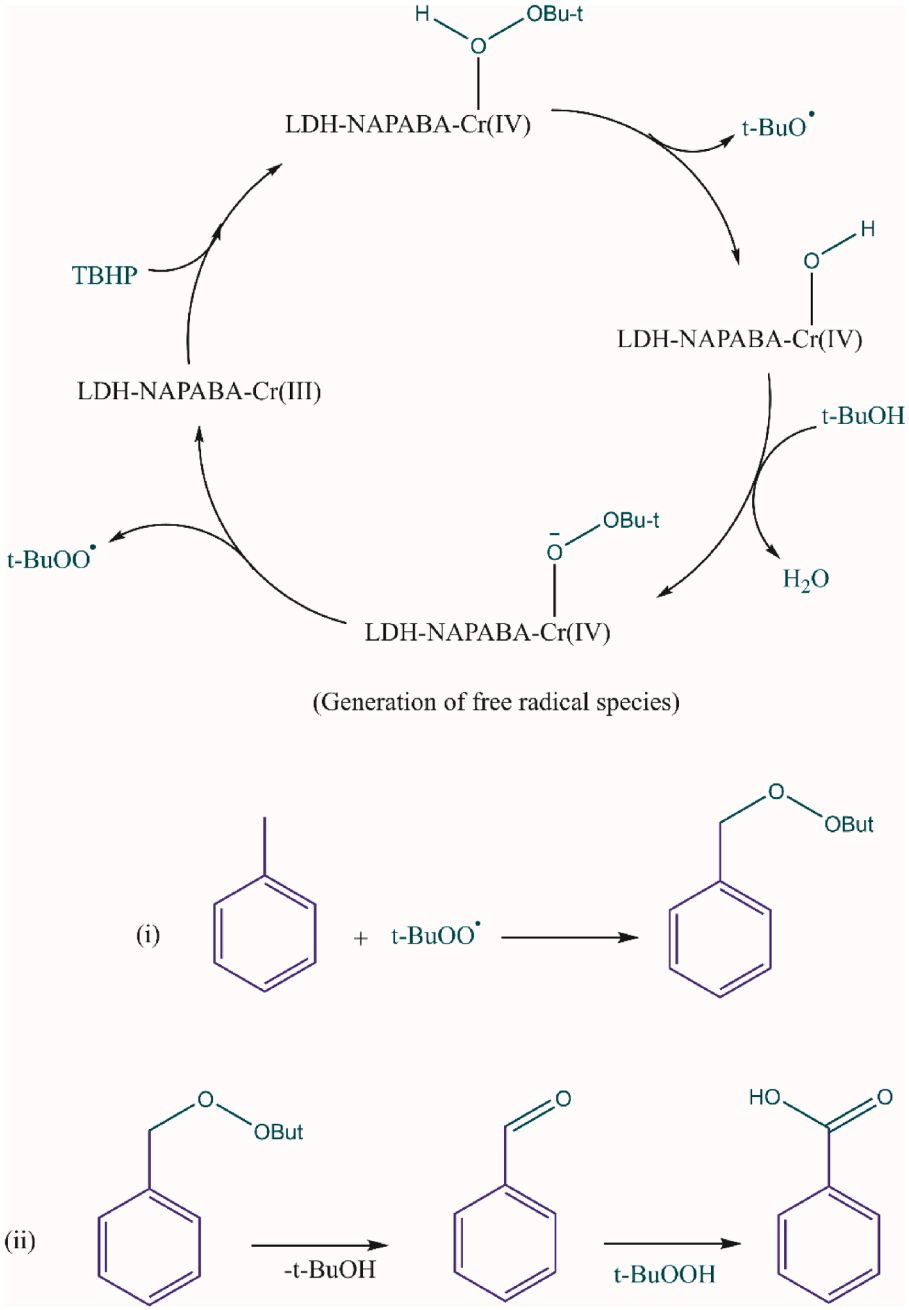

Scheme 3. The plausible mechanism for the oxidation of toluene with TBHP catalyzed by the LDH-[NAPABA-Cr(III)] catalyst.

Data availability

Data will be made available on request.

Acknowledgment

The authors are thankful UGC-DAE Consortium of Scientific Research, Devi Ahilya University Indore for providing SEM, XRD, and EDX facilities and Central Salt and Marines Chemical Research Institute (CSMCRI), Bhavnagar, Gujarat for providing BET surface area, GC-MS facilities and STIC Cochin for providing DRUV-vis facility.

Appendix A. Supplementary data

Supplementary data to this article can be found online at https://doi.org/10.1016/j.rechem.2022.100503.

References

[1] R.A. Sheldon, J.K. Kochi, Metal-Catalyzed Oxidation of Organic Compounds, Academic Press, New York, 1981.
[2] Y. Ishii, S. Sakaguchi, T. Iwahama, Adv. Synth. Catal. 343 (2001) 393–427.
[3] K. Nomiya, K. Hashino, Y. Nemoto, M. Watanabe, J. Mol. Catal. A: Chem. 176 (2001) 79–86.
[4] J. Gao, X. Tong, X. Li, H. Miao, J. Xu, J. Chem. Technol. Biotechnol. 2002 (2007) 620–625.
[5] R.L. Brutchey, I.J. Drake, A.T. Bell, T. Tilley, Chem. Commun. (2005) 3736–3738.
[6] X. Gu, C. Huang, Z. Xu, H. Wu, R. Dong, R. Liu, J. Chen, H. Zhu, J. Solid State Chem. 294 (2021), 121803.
[7] G. Song, L. Feng, J. Xu, H. Zhu, Res. Chem. Intermed. 44 (2018) 4989–4998.
[8] M. Nawab, S. Barot, R. Bandyopadhyay, New J. Chem. 43 (2019) 4406–4412.
[9] C. Huang, X. Su, D. Zhang, X. Gu, R. Liu, H. Zhu, Inorg. Chim. Acta 510 (2020), 119737.
[10] T. Xue, R. Li, Z. Zhang, Y. Gao, Q. Wang, J. Environ. Sci. 96 (2020) 194–203.
[11] Y. Zhang, H. Xu, S. Lu, RSC Adv. 11 (2021) 24254–24281.

[12] J.S. Kruger, N.S. Cleveland, S. Zhang, R. Katahira, B.A. Black, G.M. Chupka, T. Lammens, P.G. Hamilton, M.J. Biddy, G.T. Beckham, ACS Catal. 6 (2016) 1316–1328.
[13] A. Aguzzi, V. Ambrogi, U. Costantino, F. Marmottini, J. Phy. Chem. Solids 68 (2007) 808–812.
[14] S.S.C. Pushparaj, C. Forano, V. Prevot, A.S. Lipton, G.J. Rees, J.V. Hanna, U. G. Nielsen, J. Phys. Chem. C 119 (2015) 27695–27707.
[15] L. Zhang, K.N. Hui, K.S. Hui, H. Lee, Electrochim. Acta 186 (2015) 522–529.
[16] M. Mureşeanu, M. Puşcaşu, S. Şomăcescu, G. Cârjă, Catal. Lett. 145 (2015) 1529–1540.
[17] D. Bharali, R. Devi, P. Bharali, R.C. Deka, New J. Chem. 39 (2015) 172–178.
[18] S.B. Ötvös, I. Pálinkó, F. Fülöp, Catal, Sci. Technol. 9 (2019) 47–60.
[19] P. Sipos, I. Pálinkó, Catal. Today 306 (2018) 32–41.
[20] X. Wang, G. Wu, X. Liu, C. Liu, Q. Zhang, Catal. Lett. 146 (2016) 620–628.
[21] G. Varga, A. Kukovecz, Z. Kónya, L. Korecz, S. Muráth, Z. Csendes, G. Peintler, S. Carlson, P. Sipos, I. Pálinkó, J. Catal. 335 (2016) 125–134.
[22] J.S. Kirar, S. Khare, N. Tiwari, Reac. Kinet. Mech. Cat. 13 (2021) 1025–1046.
[23] J.S. Kirar, S. Khare, N. Tiwari, Chemistryselect 32 (2021) 11557–11568.
[24] J.S. Kirar, S. Khare, RSC Adv. 8 (2018) 18814–18827.
[25] K. Abderrazek, N.F. Srasra, E. Srasra, J. Chin. Chem. Soc. 64 (2017) 346–353.
[26] A.A. Sertsova, E.N. Subcheva, E.V. Yurtov, Russ. J. Inorg. Chem. 60 (2015) 23–32.
[27] A.A.A. Ahmed, Z.A. Talib, M.Z. Hussein, A. Zakaria, J. Solid State Chem. 191 (2012) 271–278.
[28] G. Wu, X. Wang, J. Li, N. Zhao, W. Wei, Y. Sun, Catal. Today, 131 (2008), pp. 402-402.
[29] K. Dutta, S. Das, A. Pramanik, J. Colloid Interf. Sci. 366 (2012) 28–36.
[30] P. Ding, B. Qu, J. Colloid Interf. Sci. 291 (2005) 13–18.
[31] M. Mamat, E. Kusrini, A.H. Yahaya, M.Z. Hussein, Z. Zainal, Int. J. Technol. 1 (2013) 73–80.
[32] S. Li, Y. Shen, M. Xiao, D. Liu, L. Fa, K. Wu, Ind. Eng. Chem. 20 (2014) 1280–1284.
[33] S. Praveen Kumar, R. Suresh, K. Giribabu, R. Manigandan, S. Munusamy, S. Muthamizh, V. Narayanan, Spectrochim. Acta Part A, 139 (2015), pp. 431.
[34] S. Khare, R. Chokhare, P. Shrivastava, J.S. Kirar, S. Parashar, J. Porous Mater. 24 (2017) 855–866.
[35] S. Khare, P. Shrivastava, J.S. Kirar, S. Parashar, Indian J. Chem. A,55 (2016) 403–412.
[36] C. Huang, X. Su, X. Gu, R. Liu. H. Zhu, Appl. Organomet. Chem. (2020), pp. e6047.
[37] W. Zhong, S.R. Kirk, D. Yin, Y. Li, R. Zou, L. Mao, G. Zou, Chem. Eng. J. 280 (2015) 737–747.
[38] C. Huang, R. Liu, W. Yang, Y. Li, J. Huang, H. Zhu, Inorg. Chem. Front. 5 (2018) 1923–1932.
[39] X. Li, L. Guo, P. He, X. Yuan, F. Jiao, Catal. Lett. 147 (2016) 856–864.
[40] Y. Zhuang, Q. Lin, L. Zhang, L. Luo, Y. Yao, W. Lu, W. Chen, Particuology 24 (2016) 216–222.
[41] X. Wang, G. Wu, H. Liu, Q. Lin, Catalysts 6 (2016) 14–23.